# Spin-charge separation in molecular wire conductance simulations

Jeremy S. Evans, Chiao-Lun Cheng, and Troy Van Voorhis
*Department of Chemistry, Massachusetts Institute of Technology, 77 Massachusetts Avenue, Cambridge, Massachusetts 02139, USA*
(Received 20 June 2008; revised manuscript received 25 August 2008; published 10 October 2008)

We analyze spin-charge separation in molecular wires using a combination of real-time density-functional simulations and model Hamiltonian calculations. By considering the *ab initio* electron dynamics of positively charged ($C_{50}H_{52}^{+}$) and negatively charged ($C_{50}H_{52}^{-}$) polyacetylene chains under a chemical potential bias, we are able to extract information about the mobility of electrons, holes, and spins in these molecules. Our results indicate that charges move more rapidly than spins in these molecules. We further supplement our *ab initio* data with empirical calculations employing the Pariser-Parr-Pople (PPP) model Hamiltonian. Our modeling indicates that the degree of spin-charge separation responds very strongly to the nonlocal exchange interaction, while showing little sensitivity to Coulombic forces. In particular, in order to reproduce the B3LYP results within the PPP model, it is necessary to reduce the strength of the exchange interaction by ca. 50% in the latter. We therefore conclude that many of the features present in the B3LYP spin current response are a direct result of self-interaction error in the functional.

DOI: 10.1103/PhysRevB.78.165108 PACS number(s): 71.10.−w, 71.15.−m, 72.25.−b

## I. INTRODUCTION

There has recently been an explosion of interest in single-molecule electronic devices resulting from a number of experiments that demonstrate their unique conductance properties.[1–27] In addition to the staircase *I-V* curves, a number of interesting effects have been observed, including Coulomb blockades,[3,11,18,28,29] negative differential resistance,[15,20,29,30] and current-driven dynamics.[21,24,31] These effects have various technological implications when considering molecular-scale devices.

As a result of this preponderance of experimental data, a significant amount of theoretical effort has recently been expended in the study of single-molecule transport. The first qualitatively correct description of this phenomenon was due to Landauer and Büttiker[32–36] in which the quantum-mechanical states of the isolated molecule become conductance channels when weakly connected to metal leads. It was quickly discovered that a Landauer-type expression could be achieved through nonequilibrium Green's function (NEGF) methods.[37–41] Although in principle the NEGF method requires the exact many-particle Hamiltonian, there have since been numerous attempts to approximate the NEGF through semiempirical,[42,43] *ab initio*,[44] density-functional theory (DFT),[45–52] and model Hamiltonian[53–55] methods.

Recently, we have proposed a method to examine single-molecule devices through real-time propagation in density-functional theory.[56] Time-dependent density-functional theory (TDDFT), based upon the seminal theorem of Runge and Gross,[57] has been both formally[58–60] and practically[61–63] applied to conduction simulations. Our method begins with a nonequilibrium initial state and propagates the state in real time using TDDFT. The electronic propagation conducts charge density through the molecular device allowing us to measure transport behavior.

In this paper we focus on the phenomenon of spin-charge separation in simple molecular wires, namely the fact that the net rates of spin and charge flow through low-dimensional systems need not be the same.[64–76] On the technological side, this effect could be exploited in spintronic devices. On the more fundamental side, spin-charge separation in molecular wires has been of theoretical interest for decades, both in the quantum chemistry community and the solid-state community. Within the solid-state community, spin-charge separation in low-dimensional systems was first proposed by Haldane[64] as a consequence of the Luttinger liquid model. Several Hubbard Hamiltonian calculations have demonstrated that in one-dimensional systems, spin and charge waves travel at different rates, with charge generally moving more rapidly than spin.[65–67] These calculations indicate that the dynamics of the up- and down-spin electrons work together to create effectively independent charge and spin dynamics.

For the specific case of conducting polymers, spin and charge behavior have been studied extensively in the static limit. Work has focused on the creation of spin- *or* charge-density waves in conjunction with the formation of a soliton, or perturbation of the bond length alternation, in polyacetylene. Solitons were initially described by Su *et al.*[77] and further studied by Bredas and Silbey[78–82] among others[83–88] using semiempirical calculations. Solitons in polyacetylene cause either spin or density waves depending on the charge of the molecule. In general, it was discovered that the spin-density waves are more localized than the charge-density waves.[80,81] While the initial studies examined systems with only spin-density waves or charge-density waves, recent theoretical[89] and experimental[90–95] studies have demonstrated both types in coexistence.

Within the transport community, the effects of spin on charge conductance have also come under scrutiny.[96] It has been recognized that spin-restricted calculations can give vastly different currents than spin-unrestricted ones,[51,97] and it is thought these differences may explain at least some part of the hundredfold discrepancy between the theory and experiments for metal-molecule-metal junction conductance. Furthermore, several studies have indicated the importance of the nonlocal exchange interaction in calculating molecular conductance.[98–103] These DFT studies indicate that the self-interaction error (SIE) produced by lack of exact exchange

 ©2008 The American Physical Society

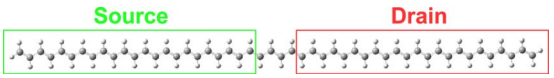


FIG. 1. (Color online) System geometry used for the DFT calculation with the source and drain labeled. The unlabeled portion is considered the molecular device. As described in the text, charge density is increased in the source and depleted in the drain before being released at $t=0$.

and the resulting charge delocalization greatly enhance conductance.

In this paper, we study the dynamics of spin-charge separation in simple polyacetylene wires using real-time propagation of the quantum wave functions. We study both the charge and spin transport due to fundamental interest in the problem and as a test case to examine the impact of various DFT approximations on each type of transport. Our primary results are obtained with TDDFT, but we also resort to a simple Pariser-Parr-Pople (PPP) model Hamiltonian in order to interpret our results and determine which effects are real and which are artifactual. We find that spin and charge can have significantly different rates of transport, even through these simple molecular wires and neglecting soliton effects. Further, we find that electron-electron interaction and SIE have profound impact on the results even at a qualitative level. In particular, we find that the large SIE present in existing density functionals radically changes the spin current characteristics of these wires. Finally, we discuss the implications of these findings for future simulations.

## II. METHODS

### A. Systems

As in our previous study,[56] we focus on the polyacetylene molecular wire $C_{50}H_{52}$ as a simple example of a conjugated molecule that supports electron transport. As shown in Fig. 1, we divide the system into an electronic source, a molecular device, and an electronic drain. This system division mirrors our previous work and much work involving molecular electronic devices.[41,42,45,48,50,56,62,104–111] We define the molecular device to be composed of four carbon atoms and their associated hydrogen atoms. Thus, the source-device-drain division is $C_{23}H_{24}$-$C_4H_4$-$C_{23}H_{24}$. Note that in this calculation, we are using a closed system to approximate the current of an open system, which is appropriate only for short times.[56] We use the $6-31g^*$ basis set and either Hartree-Fock (HF) (which contains 100% exact exchange but no correlation) or the B3LYP functional (which contains some correlation but only 20% exact exchange). Unlike in previous applications, we simulate the cation ($C_{50}H_{52}^+$) and the anion ($C_{50}H_{52}^-$) rather than the neutral chain. Since these chains now contain an *odd* number of electrons the system will always have a net spin polarization and we can independently consider the rates of spin and charge transport through the wire as the voltage is applied.

### B. Real-time density-functional conductance simulations

Our primary means of obtaining conductance information on these wires exploits the real-time density-functional theory (TDDFT) propagation code developed recently in our group. The details of this approach are presented elsewhere,[56] and so here we present only the necessary points. Briefly: contrary to our previous work, we now include both charge and spin constrained initial conditions with spin-unrestricted propagation.

As described above and in Fig. 1, we divide the system into an electronic source, molecular device, and an electronic drain. In this work, we examine properties that can be described using the total density difference ($N_{\mathrm{tot}}$) and spin-density difference ($M_{\mathrm{spin}}$) in the source and drain. We make the following definitions of $N_{\mathrm{tot}}$ and $M_{\mathrm{spin}}$:

$$N_{\mathrm{tot}} = (n_S^{\uparrow} + n_S^{\downarrow}) - (n_D^{\uparrow} + n_D^{\downarrow}), \tag{1}$$

$$M_{\mathrm{spin}} = (n_S^{\uparrow} - n_S^{\downarrow}) - (n_D^{\uparrow} - n_D^{\downarrow}), \tag{2}$$

where the variables $n_S^{\uparrow}$, $n_D^{\uparrow}$, $n_S^{\downarrow}$, and $n_D^{\downarrow}$ represent the number of charges of each spin ($\uparrow,\downarrow$) in the source (S) and drain (D).

The initial state of the system is determined by constrained DFT.[112,113] We want to control the values of $N_{\mathrm{tot}}$ and $M_{\mathrm{spin}}$ defined in Eqs. (1) and (2). For each of $n_S^{\uparrow}$, $n_D^{\uparrow}$, $n_S^{\downarrow}$, and $n_D^{\downarrow}$ in the above equations, we can define an associated operator—$n_S^{\uparrow}(\mathbf{r})$, $n_D^{\uparrow}(\mathbf{r})$, $n_S^{\downarrow}(\mathbf{r})$, $n_D^{\downarrow}(\mathbf{r})$—that measures the appropriate number of electrons using the Becke weight definition. Then, we define operators $N_{\mathrm{tot}}(\mathbf{r}) \equiv n_S^{\uparrow}(\mathbf{r}) + n_S^{\downarrow}(\mathbf{r}) - n_D^{\uparrow}(\mathbf{r}) - n_D^{\downarrow}(\mathbf{r})$ and $M_{\mathrm{spin}}(\mathbf{r}) \equiv n_S^{\uparrow}(\mathbf{r}) - n_S^{\downarrow}(\mathbf{r}) - n_D^{\uparrow}(\mathbf{r}) + n_D^{\downarrow}(\mathbf{r})$ and associate with each a Lagrange multiplier—$V_{\mathrm{tot}}$ or $V_{\mathrm{spin}}$. Our desire is to find an initial state that has a prescribed set of $N_{\mathrm{tot}}$ and $M_{\mathrm{spin}}$ values. We enforce this by extremizing

$$W[\rho, V_{\mathrm{tot}}, V_{\mathrm{spin}}] = E[\rho] + V_{\mathrm{tot}}\left(\int N_{\mathrm{tot}}(\mathbf{r})\rho(\mathbf{r})d\mathbf{r} - N_{\mathrm{tot}}\right) + V_{\mathrm{spin}}\left(\int M_{\mathrm{spin}}(\mathbf{r})\rho(\mathbf{r})d\mathbf{r} - M_{\mathrm{spin}}\right), \tag{3}$$

where $E[\rho]$ is the DFT energy functional, and each subsequent term enforces one of the particle number constraints. The terms $V_{\mathrm{tot}}N_{\mathrm{tot}}(\mathbf{r})$ and $V_{\mathrm{spin}}M_{\mathrm{spin}}(\mathbf{r})$ act as *chemical potentials* that adjust the charge and spin number differences between the leads. These potentials are nonzero in the regions of space close to the leads in question and have opposite signs on the source and drain. Due to the conjugate relationship between the numbers and their Lagrange multipliers we can use either a chemical potential (e.g., $V_{\mathrm{tot}}$) or a number (e.g., $N_{\mathrm{tot}}$) as our independent variable in what follows. In choosing initial conditions, we choose systems with integer values of $N_{\mathrm{tot}}$ and $M_{\mathrm{spin}}$.

At time $t=0$, we release the chemical potentials, creating a state with a nonequilibrium distribution of charge and electronic spin. Although this turn-off is abrupt, our previous work[56] indicates that a turn-off with time scale as slow as $\tau \approx 0.35$ fs gives essentially the same results. The system is propagated according to the one-particle time-dependent Kohn-Sham (KS) equations,[57]

$$\hat{H}[\rho^{\uparrow}, \rho^{\downarrow}]_{\mathrm{KS}}^{\uparrow}\psi_a^{\uparrow}(t) = i\hbar\frac{\partial\psi_a^{\uparrow}(t)}{\partial t},$$

$$\hat{H}[\rho^{\uparrow},\rho^{\downarrow}]^{\downarrow}_{\mathrm{KS}}\psi^{\downarrow}_{a}(t) = i\hbar\frac{\partial\psi^{\downarrow}_{a}(t)}{\partial t}, \tag{4}$$

where $\rho^{\uparrow(\downarrow)}(t)=\Sigma_a^{occ}|\psi_a^{\uparrow(\downarrow)}(t)|^2$. Notice that Eq. (4) propagates each spin channel separately (i.e., it is spin unrestricted) and that the propagations are coupled, because the effective Hamiltonians depend on both the ↑ and ↓ densities simultaneously. The KS effective Hamiltonians are constructed using readily available adiabatic approximations to their exact forms.[114] The numerical solution to Eq. (4) follows our previous work[56] with the second-order Magnus propagator.

As the density matrix is propagated, we record the up- and down-spin densities on each lead; the source, and the drain. We determine time-dependent populations—$n_S^{\uparrow}(t)$, $n_S^{\downarrow}(t)$, $n_D^{\uparrow}(t)$, $n_D^{\downarrow}(t)$—using the Löwdin population definition. From these populations, we calculate transient currents by averaging the time derivatives of the number variables over some time interval $\Delta t$. Thus,

$$I_{\mathrm{tot}}(t) = \frac{N_{\mathrm{tot}}(t+\Delta t/2) - N_{\mathrm{tot}}(t-\Delta t/2)}{2\Delta t}, \tag{5}$$

$$I_{\mathrm{spin}}(t) = \frac{M_{\mathrm{spin}}(t+\Delta t/2) - M_{\mathrm{spin}}(t-\Delta t/2)}{2\Delta t}, \tag{6}$$

where $N_{\mathrm{tot}}$ and $M_{\mathrm{spin}}$ are defined by Eqs. (1) and (2). To obtain essentially steady-state currents, we set $\Delta t=0.48$ fs, which is significantly larger than the propagation time step.[56] We choose a unique current for a given voltage by taking the maximum current achieved in the steady-state region. In general, the maximum current is reached between 0.5 and 1 fs.[56]

The method summarized above provides several strengths compared to commonly used current calculation techniques. First, the accuracy-cost tradeoff of the propagation can be controlled by adjusting the calculation parameters: time step, size of leads, and propagation duration. In this way, one can make a controlled approach to the infinite system limit without unnecessary approximations. Second, using a Gaussian basis allows us to easily include the effects of exact exchange in the dynamics and therefore in the current determination. Finally, the use of the single-particle KS Hamiltonian to propagate the single-particle density of a closed system is rigorously supported by TDDFT. Meanwhile the use of the same Hamiltonian in nonequilibrium Green's function methods is somewhat *ad hoc*.

On the other hand, our TDDFT method presents some practical difficulties in predicting steady-state currents. First, the technique is expensive compared to currently available NEGF techniques. In constructing a current-voltage curve, each data point requires a separate initial state and propagation with little work reusable from point to point. For $C_{50}H_{52}$, each B3LYP propagation of 125 time steps took approximately 2.5 days on a single processor. Additionally, these techniques have not yet been extended to open systems. Therefore, the long time dynamics do not reflect the behavior of a real system with *de facto* infinite leads and electron reservoirs. Even with these difficulties, however, real-time propagation provides a promising means to predict the current of a system under an external potential.

### C. Empirical model Hamiltonians

To interpret our results, we found it useful to fit our TDDFT data to simple, parametrized, semiempirical Hamiltonians representing the conjugated $\pi$ backbone of our molecule. These techniques have been used extensively to study charge transport in organic molecules in the past.[42,43,115–117] The difference here is that in our calculations the model parameters are determined *post hoc* from the DFT data. Thus, the model Hamiltonian is tailored to give a charge-transfer energy landscape that is as close as possible to the TDDFT results. The goal is to develop a simplified system that displays similar behavior to the DFT simulations described above. However, by reducing the number of degrees of freedom, we are able to perform calculations *much more quickly* allowing us to test, for example, a larger range of voltages, and to better understand the physics involved.

We use the PPP Hamiltonian[118,119] with electron-electron interaction defined by the Mataga-Nishimoto[120,121] formula. Neglecting nuclear-nuclear interaction, the Hamiltonian takes the form

$$\hat{H} = -\beta\sum_{j}^{N-1}\sum_{\sigma=\uparrow,\downarrow}(\hat{c}^{\dagger}_{j,\sigma}\hat{c}_{j+1,\sigma} + \hat{c}^{\dagger}_{j+1,\sigma}\hat{c}_{j,\sigma}) - \sum_{j,k}^{N}\Gamma_{j,k}\hat{n}_j + \frac{1}{2}\sum_{j,k}\Gamma_{j,k}\hat{n}_j\hat{n}_k,$$

$$\Gamma_{j,k} = \left(r_0|j-k| + \frac{1}{g}\right)^{-1}. \tag{7}$$

In these equations, the summation indices $j$ and $k$ refer to position along the chain. The operator $\hat{n}_j \equiv (\hat{c}^{\dagger}_{j,\uparrow}\hat{c}_{j,\uparrow} + \hat{c}^{\dagger}_{j,\downarrow}\hat{c}_{j,\downarrow})$ is the number operator on the $j$th position. The terms in Eq. (7) from left to right are the kinetic energy, the electron-nuclear attraction, and the electron-electron repulsion. The parameters in the model Hamiltonian are the C–C bond distance ($r_0=2.647$), the adjacent site hopping parameter ($\beta$), and the same site electronic interaction strength ($g$). This leaves the values of $\beta$ and $g$ to be set as parameters. To model the 50 carbon chain under study in this work, we set $N=50$. We model the anion or cation by considering 51 or 49 electron systems, respectively.

We use an unrestricted Hartree-Fock prescription for the wave function, which yields the energy

$$E[\mathbf{P}] = -\beta\sum_{j}^{N-1}(P^{\uparrow}_{j,j+1} + P^{\downarrow}_{j,j+1} + P^{\uparrow}_{j+1,j} + P^{\downarrow}_{j+1,j}) - \sum_{j,k}^{N}\Gamma_{j,k}(P^{\uparrow}_{j,j} + P^{\downarrow}_{j,j}) + E_J[\mathbf{P}] - E_K[\mathbf{P}],$$

$$E_J[\mathbf{P}] = \frac{1}{2}\sum_{j,k}^{N}\Gamma_{j,k}(P^{\uparrow}_{j,j} + P^{\downarrow}_{j,j})(P^{\uparrow}_{k,k} + P^{\downarrow}_{k,k}),$$

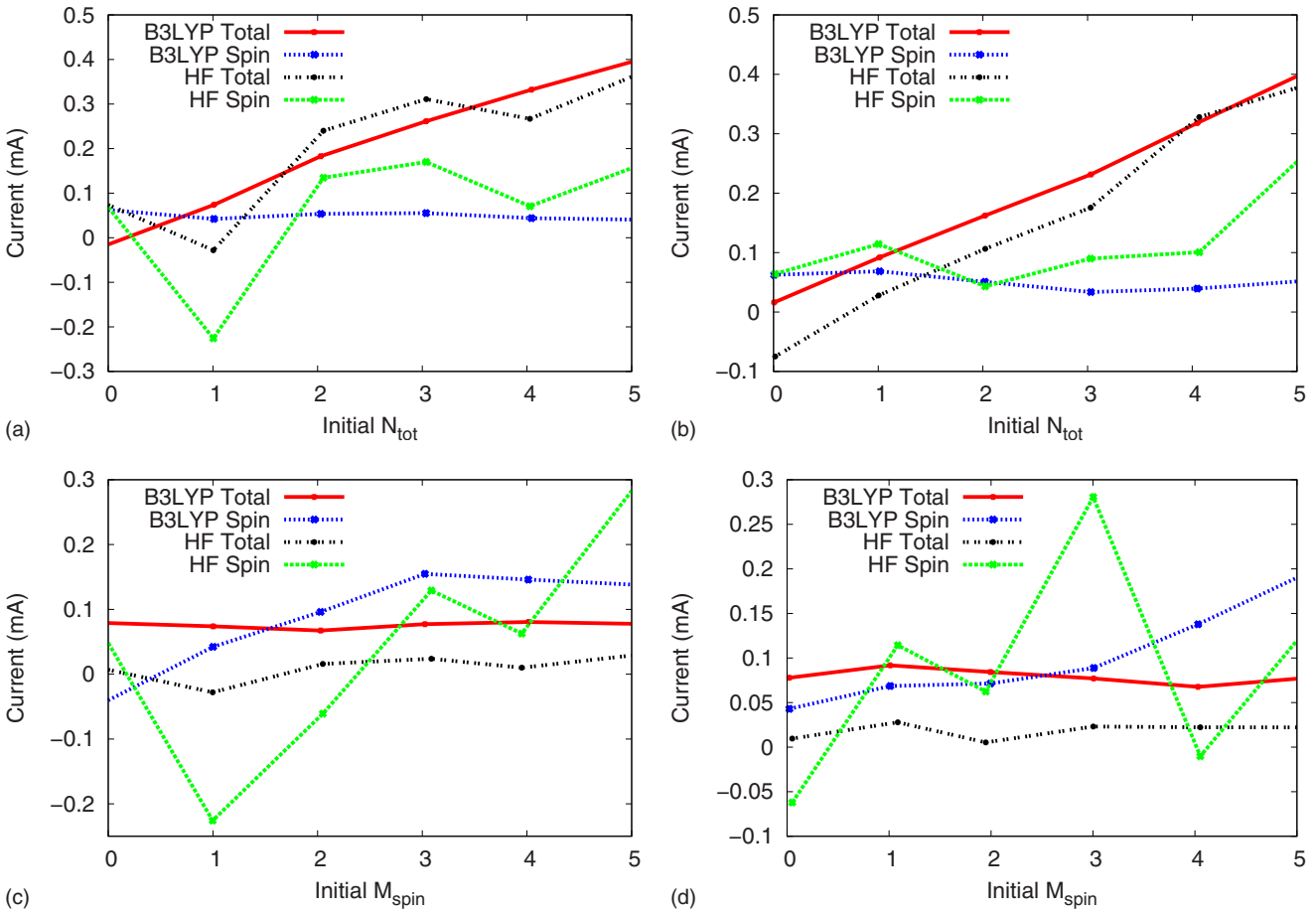


FIG. 2. (Color online) Plot of $I_{\mathrm{tot}}$ and $I_{\mathrm{spin}}$ as a function of initial $N_{\mathrm{tot}}$ and $M_{\mathrm{spin}}$ as determined using B3LYP or HF for the anion (left) and cation (right) case. The value of the fixed initial $M_{\mathrm{spin}}$ or $N_{\mathrm{tot}}$ is set to 1.0.

$$E_K[\mathbf{P}] = \frac{1}{2}\sum_{j,k}^{N} \Gamma_{j,k}(P^{\uparrow}_{j,k}P^{\uparrow}_{k,j} + P^{\downarrow}_{j,k}P^{\downarrow}_{k,j}), \tag{8}$$

where $\mathbf{P}$ is the one-particle density matrix with separate up- and down-spin parts and $E_J$ and $E_K$ are the Coulomb and exchange energies, respectively.

We calculate currents in the PPP model using a method analogous to that used for our TDDFT calculations: an initial nonequilibrium state is prepared in the presence of independent chemical potentials on the leads, and the potentials are released at time $t=0$. Defining the Fock operators

$$\hat{F}^{\uparrow(\downarrow)}[\mathbf{P}] \equiv \frac{\partial E[\mathbf{P}]}{\partial \mathbf{P}^{\uparrow(\downarrow)}}, \tag{9}$$

we propagate the system via time-dependent HF,

$$\hat{F}^{\uparrow}[\mathbf{P}]\psi^{\uparrow}(t) = i\hbar\frac{\partial \psi^{\uparrow}(t)}{\partial t},$$

$$\hat{F}^{\downarrow}[\mathbf{P}]\psi^{\downarrow}(t) = i\hbar\frac{\partial \psi^{\downarrow}(t)}{\partial t}, \tag{10}$$

similar to TDKS. The propagation is performed with the second-order Magnus method,[56] populations $\{n_S^{\uparrow}(t), n_S^{\downarrow}(t), n_D^{\uparrow}(t), n_D^{\downarrow}(t)\}$ are determined by the Löwdin definition, and currents are determined by Eqs. (5) and (6).

Several variations of the Hamiltonian and parameters will be useful in what follows. In particular, we will introduce SIE into the PPP model (PPP-SIE). SIE is the unphysical Coulombic repulsion one electron feels due to its own charge distribution.[122] This repulsion is exactly canceled by the exchange interaction, but since most functionals treat exchange approximately, there is always some residual SIE in a functional like B3LYP. To introduce analogous SIE into the PPP model, we multiply the exchange component of the PPP energy [Eq. (8)] by $a_X=0.5$ so that the exchange and Coulomb pieces no longer cancel. Additionally we performed PPP model calculations in the Hartree (PPP-Hartree, $a_X=0$) and Hückel ($g\to 0$) approximations which neglect, respectively, all exchange and all electron-electron repulsion.

## III. RESULTS

### A. Real-time TDDFT currents

In Fig. 2 we present the TDB3LYP and TDHF spin and charge currents as a function of initial $N_{\mathrm{tot}}$ with fixed initial $M_{\mathrm{spin}}=1$ and as a function of initial $M_{\mathrm{spin}}$ with fixed initial $N_{\mathrm{tot}}=1$. We choose to present currents as a function of initial distribution to directly compare charge and spin behavior even though this choice does not allow a direct calculation of

conductance. Focusing first on the DFT results, we see that the charge current increases nearly linearly with the initial $N_{\mathrm{tot}}$. Under the same circumstances, spin current is nearly constant showing only very small dependence on initial $N_{\mathrm{tot}}$. Also as expected, the spin current generally increases with increased initial $M_{\mathrm{spin}}$. However, for spin the trend is much less linear than it is for charge. We also see nonzero spin currents for initial $M_{\mathrm{spin}}=0$. Although this is initially surprising, we must remember that the propagation is not beginning from an equilibrium initial state because $N_{\mathrm{tot}}\neq 0$, so some spin motion can be expected. Finally, just as $N_{\mathrm{tot}}$ weakly influenced spin current, so $M_{\mathrm{spin}}$ has little effect on the charge current.

The B3LYP results in Fig. 2 agree with known properties of spin-charge separation. For the case of $M_{\mathrm{spin}}=N_{\mathrm{tot}}=1$, the charge current is larger than the spin current. This occurs despite the fact that the initial charge and spin differences are equivalent. Similarly, the total current for a particular value of $N_{\mathrm{tot}}$ is larger than the spin current for that value of $M_{\mathrm{spin}}$. For example, for $M_{\mathrm{spin}}=N_{\mathrm{tot}}=1$ we have $I_{\mathrm{tot}}/I_{\mathrm{spin}}=1.7$ for the anion and $I_{\mathrm{tot}}/I_{\mathrm{spin}}=1.3$ for the cation. This behavior has been shown previously in correlated systems.[65–67] In correlated calculations, one measures charge and spin-wave velocity in the Hubbard model to give $v_{\mathrm{tot}}/v_{\mathrm{spin}}=1$ with no on-site electron-electron interaction ($g=0$) and $v_{\mathrm{tot}}/v_{\mathrm{spin}}\approx N_e$ with large on-site electron-electron interaction ($g\geq 10\beta$) where $N_e$ is the number of electrons. As we will see in Sec. III B, the B3LYP propagation is best modeled with $g=3.4\beta$. Thus, the charge-spin current ratio falls between the zero electron-electron repulsion and the large repulsion limit as we expect.

Turning our attention to the Hartree-Fock calculated currents, we note that both the spin and charge currents calculated with the Hartree-Fock functional fluctuate more as a function of particle number than those calculated with B3LYP. We will see in Sec. III C that these fluctuations result from exact exchange in the HF functional. While the nonmonotonic nature of the data makes determining trends for the spin currents impossible with the data available, the charge currents approximately follow the trends established by B3LYP. We note that, while previous investigations have demonstrated the effect of HF exchange on the *magnitude* of the current predicted at low bias,[98,99,102,123] this work presents an example of the effect of HF exchange on the qualitative shape of the current-bias curve.

### B. Obtaining model Hamiltonian parameters

We have empirically fit the PPP model parameters, $\beta$ and $g$, to reproduce the equilibrium behavior of DFT under various chemical potential biases. The parameters are adjusted until the two methods show approximate agreement for the values of $N_{\mathrm{tot}}$ and $M_{\mathrm{spin}}$ over the range $-8<V_{\mathrm{tot}}<8$ and $-1.5<V_{\mathrm{spin}}<1.5$. Note that we are using PPP as an interpretive tool, rather than a quantitative analysis technique. Thus, we adjust $\beta$ and $g$ by visual inspection and do not concern ourselves with numerical fitting. The fitting for two different parameters was aided by the empirical observation that $g$ primarily influenced the slope of the $N_{\mathrm{tot}}$ versus $V_{\mathrm{tot}}$ plot while only $\beta$ affects the slope of $M_{\mathrm{spin}}$ versus $V_{\mathrm{spin}}$. The parameters chosen were $\beta=0.16$ and $g=0.55$. These values are not too far off the values of $\beta=0.0878$ and $g=0.398$ suggested by Mataga and Nishimoto.[121] The charge and spin number versus potential plots for the cation and anion are shown in Fig. 3. Clearly the parameters chosen give the correct overall slope to these plots. Furthermore, the steplike nature of HF is reproduced by PPP. However, the B3LYP results show smooth dependence of $N_{\mathrm{tot}}$ on $V_{\mathrm{tot}}$ while PPP and HF produce steps. We note that the steplike behavior of PPP was not influenced in any way by the parameter choice.

The reason for the differences between PPP and B3LYP is relatively simple: for PPP one is using a SIE-free HF prescription for the energy, while B3LYP includes spurious self-interaction terms. This distinction is important because it has been shown that SIE can have a profound effect on charge transfer, current dynamics, and spin states.[101,124,125] The same is true in this case, as artificially reducing the exchange term in PPP by 50% (PPP-SIE) improves agreement with B3LYP in the static potential-dependent $N_{\mathrm{tot}}$ and $M_{\mathrm{spin}}$. The PPP-SIE method produces nearly linear results for total density, and step behavior for the spin density in agreement with B3LYP. We have run similar calculations with PPP-Hartree (0% exact exchange) and find near-linear particle number versus potential behavior for *both* charge and spin. On the other hand, Fig. 3 shows that full PPP (100% exchange) produces steps for both total and spin density. Only with *partial* cancellation of the SIE (as with PPP-SIE) can we obtain qualitative agreement with the B3LYP data.

The self-interaction-induced smoothing of the $N_{\mathrm{tot}}$ versus $V_{\mathrm{tot}}$ steps has previously been reported by Baer *et al.*[126] for weakly coupled subsystems and is known to reflect the tendency of SIE to favor charge delocalization. Here we see that these steps persist even in a molecular wire that is strongly coupled to the leads. Steps also occur for spin distribution, reflecting *spin* localization as well. The small amount of exact exchange in B3LYP predicts the unusual situation of spin *localization* together with charge *delocalization*. This unusual localization-delocalization situation is closely coupled to the transport predictions in Sec. III A.[123]

### C. Model Hamiltonian currents

The PPP current versus number plots are shown in Fig. 4. As expected from the static calculations in Sec. III B the full PPP currents resemble those calculated by HF while PPP-SIE gives much better qualitative agreement with B3LYP. In addition to PPP-SIE ($a_X=0.5$), PPP-Hartree ($a_X=0$) and Hückel ($g\rightarrow 0$) results are also included in Fig. 4. We first examine the charge currents. With PPP-SIE charge currents increase essentially monotonically while the PPP calculated current profile fluctuates. Furthermore, we notice that PPP-Hartree and PPP-SIE agree almost quantitatively for charge currents. This suggests that below a certain threshold (i.e., with less than 50% exchange), exchange has little impact on charge current. From the comparison of Hückel and PPP-Hartree we also see that removing the Coulomb interaction significantly reduces charge current, so that a noninteracting picture of these wires is inadequate.

Considering spin properties, we see that for PPP-SIE there is only one small region of nonmonotonic behavior (in

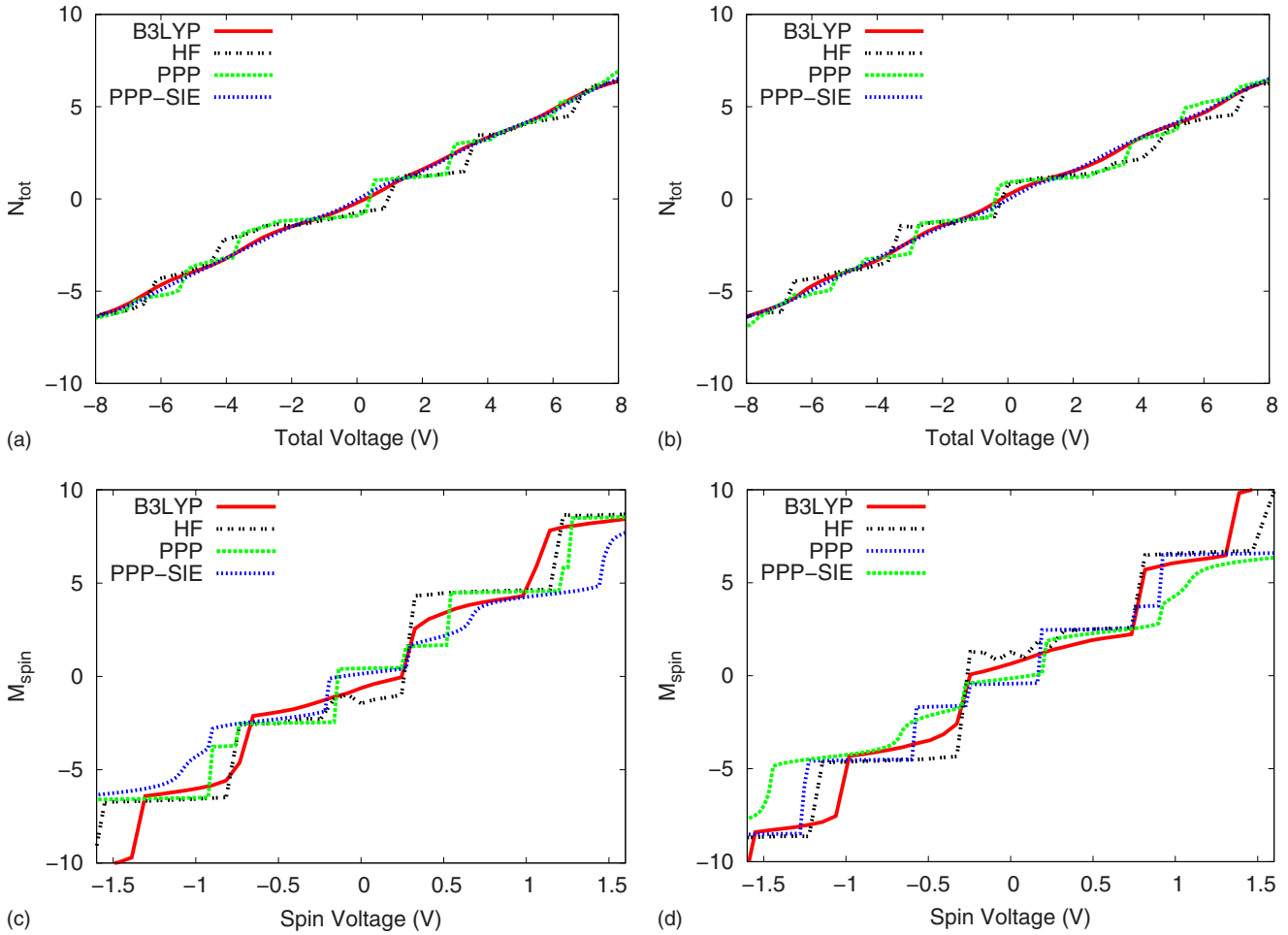


FIG. 3. (Color online) Dependence of $N_{tot}$ upon $V_{tot}$ with $V_{spin}=0.272V$ and $M_{spin}$ upon $V_{spin}$ with $V_{tot}=1.36V$ for the anion (left) and cation (right) as predicted by B3LYP, PPP, and PPP-SIE.

the anion spin current plot at initial $M_{spin}=1$). On the other hand, PPP produces fluctuating spin current profiles such that even determining a trend is difficult. Meanwhile, the spin current plots are nearly identical for PPP-Hartree and Hückel propagation. Thus, we see that the exchange interaction is much more important than the Coulombic interaction in determining spin transport. The importance of the exchange piece over the Coulomb piece can be explained by realizing that the Coulomb interaction acts between any two electrons regardless of spin while the exchange interaction only acts between electrons of the same spin. Thus, changing the spin density while allowing the charge density to remain the same by switching an up- and down-spin electron will change exchange energy, but not Coulomb. We thus see that the phenomenon of spin-charge separation is inextricably linked to the description of electronic exchange. The deep connection between spins and currents in TDDFT has been addressed previously in a completely different context.[127,128]

Examining the time series data (not shown) reveals that a major source of the erratic current behavior in PPP and HF is that these full exchange propagations do not always relax toward symmetric charge and spin distributions. As an example, for the anion with initial $N_{tot}=M_{spin}=1$, Hartree-Fock predicts relaxation toward $N_{tot}\approx 1$ and $M_{spin}\approx 2.3$ resulting in near 0 charge current and negative spin current as shown in Fig. 2. This unusual behavior does not occur with B3LYP or PPP-SIE. The tendency of exact exchange methods to relax toward broken symmetry charge or spin densities is likely related to the steplike behavior of the $N_{tot}$ and $M_{spin}$ dependence on $V_{tot/spin}$ in that both seem to indicate local minima in the electronic potential energy surface other than the symmetric distribution. Indeed, such charge and spin localization are known to be favored by exact exchange.

## IV. DISCUSSION

Note that the PPP model is computationally inexpensive, so we can perform analogous calculations on much longer wires, allowing us to approach the thermodynamic limit. To demonstrate this, we show in Fig. 5 the PPP-SIE calculated current versus potential plots for the carbon chains of lengths 50, 100, and 200 with a fixed molecule segment of four sites. We have chosen potential rather than number as our independent variable because the former is size intensive, facilitating the comparison of different length chains. For both the charge and spin plots, the slopes remain the same with increasing chain length, converging to a junction conductance of about $0.5G_0$ for charges, but $1.2G_0$ for spins, in qualitative

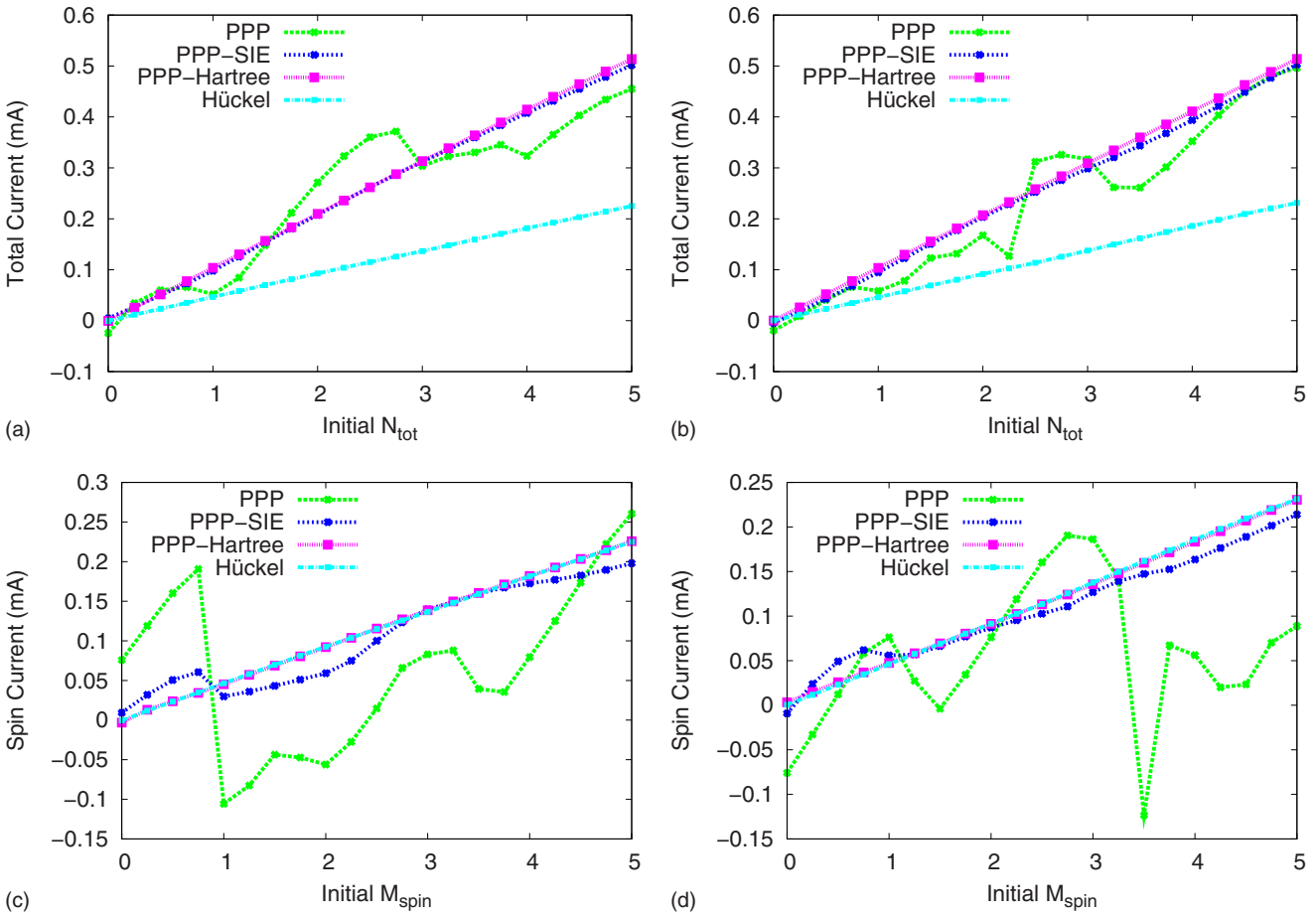


FIG. 4. (Color online) Maximum total and spin currents plotted against initial $N_{\mathrm{tot}}$ and $M_{\mathrm{spin}}$, respectively, as calculated by PPP, PPP-SIE, PPP-Hartree, and Hückel propagation for the anion (left) and cation (right). The unvaried initial $N_{\mathrm{tot}}$ or $M_{\mathrm{spin}}$ is held to 1.0.

agreement with previous simulations.[56] We thus see the unusual fact that while an *individual* spin moves more slowly than an individual charge by a factor of $I_{\mathrm{charge}}/I_{\mathrm{spin}} \approx 1.3-1.7$ (vide infra) yet the molecular conductivity for spins is higher because less potential needs to be applied to separate spins as opposed to charges.

Another interesting point is that increasing chain length produces more closely spaced steps in the *I-V* plot. This can be explained by considering that an increase in chain length means that a given potential transfers more whole electrons from one side to the other creating more steps. These results suggest that one may regain a smooth spin *I-V* curve in the infinite chain limit. We could easily repeat these calculations using any of our PPP methods, but at the moment we simply wish to demonstrate that large chain calculations are possible with the model Hamiltonian used in this study.

The TDDFT calculations presented in this paper suggest that for one-dimensional systems, charge and spin do indeed behave as separate quasiparticles. This separation is seen most clearly in that, for B3LYP, charge transport occurs more quickly than spin transport from analogous initial states in agreement with the results of correlated real-time model system simulations.[65–67] Hartree-Fock shows large fluctuations in the current profiles for charge and spin, making it difficult to assess which quasiparticle travels more quickly. Similarly, spin and charge show different particle number versus potential behavior as seen in Fig. 3. Both the greater step behavior in Fig. 3 and reduced transport properties of spin relative to charge relate to the greater localization of spin over charge demonstrated in studies of density waves caused by solitons.[80,81] The tendency of charge to delocalize increases the probability of partial charges on the right and left leads of the system. Furthermore, the same forces that cause electrons to delocalize also cause charge to travel more quickly than spin.

We have demonstrated real-time transport calculations in which DFT with the B3LYP functional and Hartree-Fock produce qualitatively different results. This presents an interesting exploration opportunity because density-functional theory and Hartree-Fock both present certain advantages for predicting transport. It is well known that Hartree-Fock is free of self-interaction error. Several previous studies have indicated that removing SIE may also significantly reduce electron transport across a molecular device.[98,99,102] Given the often 1 to 2 orders of magnitude overestimate of charge currents from existing DFT calculations, one would thus be tempted to conclude that a method like HF might offer some distinct advantages. On the other hand, Hartree-Fock clearly lacks important pieces of the Hamiltonian. The single-determinant picture includes no correlation, while modern density functionals contain at least an approximate correlation energy. These semilocal correlation functionals allow

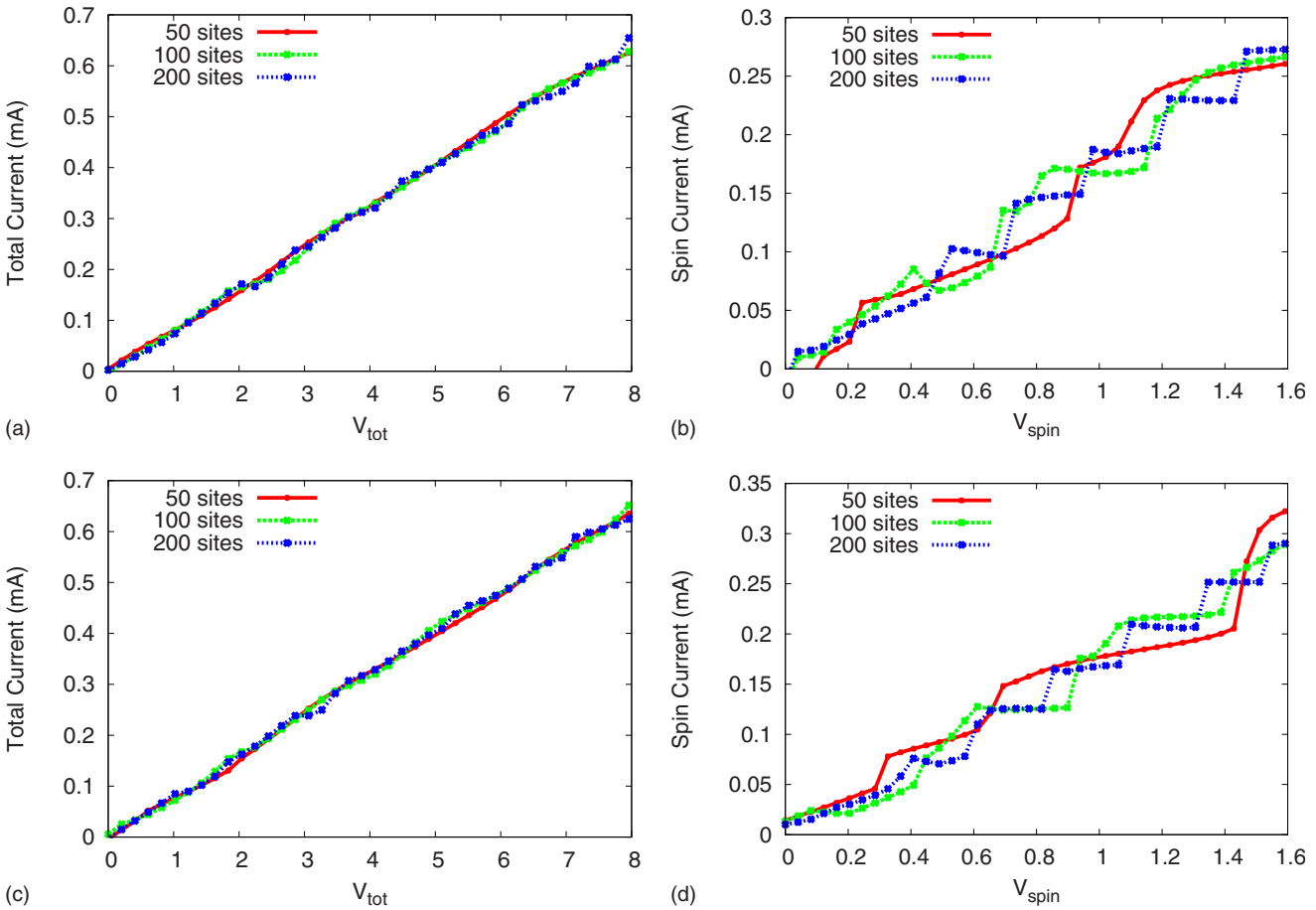


FIG. 5. (Color online) Maximum total and spin currents plotted against initial $V_{tot}$ and $V_{spin}$, respectively, as calculated by PPP-SIE, for chains of lengths 50, 100, and 200 sites. The fixed initial potentials are $V_{spin}=0.272V$ for the total current plots and $V_{tot}=1.36V$ for the spin current plots.

modern DFT to predict energies with surprising accuracy, even in the presence of SIE. The cancellation of errors which leads to accurate equilibrium properties in DFT may also contribute to accuracy in transport simulations. Specifically, it is known that describing density of state alignment between the leads and device is very important in describing transport properties.[100] Furthermore, recent studies[98] indicate that Hartree-Fock greatly overestimates the highest occupied molecular orbital-lowest unoccupied molecular orbital (HOMO-LUMO) gap resulting in artificially reduced conductance properties, while B3LYP provides more consistent energy gaps, potentially leading to more reliable currents. In order to resolve which method is actually closer to reality for these systems, one would really need to perform correlated *ab initio* calculations. Such simulations are outside the scope of this work, but would certainly advance the field.

The questions posed in regards to the impact of exchange and correlation on modeling transport are critical due to the large difference between theory and experiment in these studies. Numerous potential sources of this difference exist. Those sources include self-interaction error from less than 100% exact exchange as discussed in this paper or correlation effects. Additionally, recent theoretical evidence[104] indicates the powerful impact that contact atomic geometry can have on the electronic transmission function, and therefore conductance. NEGF methods may also develop errors in the use of an equilibrium single-particle Fock matrix as a substitute for the nonequilibrium many-particle Hamiltonian. With all these potential sources of error, it is necessary to clarify the impact of each of these approximations.

Our work clarifies the differences in *both* charge and spin behaviors when calculated with 100% exact exchange (Hartree-Fock, PPP) compared to calculations with less than 100% exact exchange (B3LYP, PPP-SIE). With exact exchange, we see results associated with localization, while introducing SIE tends to favor delocalized, partial charge and spin states. In particular, we see that localization effects are enhanced in spin transport simulations relative to charge transport. We propose this sensitivity of spin transport properties can act as a measure of how well exchange properties are described by a particular method.

## V. CONCLUSIONS

We have analyzed real-time spin and charge currents through polyacetylene wires using TDDFT. Our calculations agree that spin and charge do indeed behave as separate particles, with charges moving faster than spins by a factor of between 1.3 and 1.7. We find that the spin dynamics in particular are critically sensitive to the nonlocal exchange inter-

action, as TDB3LYP and TDHF show qualitatively different behavior for the spin dynamics. The former shows a smooth, essentially monotonic increase in spin current as the initial $M_{\text{spin}}$ is increased, while the latter shows fluctional and even negative currents as a function of $M_{\text{spin}}$. Meanwhile, the charge currents are primarily modulated by the strength of the classical Coulomb repulsion. We find empirically that the TDB3LYP dynamics can be well reproduced by a simple PPP model if we artificially introduce some self-interaction error into the PPP model by reducing the amount of nonlocal exchange by 50%. Conversely, PPP without SIE reproduces the fluctuating behavior of TDHF. Thus, we see that methods with 100% exact exchange give qualitatively different results as regards spin/charge separation from those with some amount of self-interaction. The enhanced influence of the exchange force on the shape of the spin current-voltage curve has not previously been noted and we propose that this could be a powerful tool for calibrating exchange-correlation functionals for transport calculations.

These results call into question the accuracy of using existing functionals for the prediction of currents in open shell systems and may help explain the erroneously large currents predicted in metal-molecule-metal junctions. Few functionals include 100% exact exchange which seems to significantly impact charge and especially spin transport. On the other hand, Hartree-Fock, which includes exact exchange, does not include correlation. It is unclear how the inclusion of both exact exchange and correlation will impact our transport results, but the two effects together may give much better agreement with experiment than we have so far seen in single-molecule charge transport calculations.

In the future, we plan to study in more detail the influence of the choice of functional, and hence the degree of SIE, on currents. In particular, we plan to examine the utility of long-range corrected functionals[129,130] for simulating conductance. Also, it would be interesting to perform some correlated *ab initio* calculations on these wires in order to determine the correct answer in cases where SIE has a significant impact. It may be the case that SIE mimics the effects of correlation. On the other hand, we may find that the SIE-free results are more appropriate, or that neither result is to be trusted. As a first approximation, we might seek to answer these questions by performing the correlated calculations on the model PPP Hamiltonian as the simplicity of the PPP model would make such calculations computationally feasible. Finally, it will be interesting to see how these results translate to more realistic lead-molecule-lead structures.

## ACKNOWLEDGMENTS

T.V.V. gratefully acknowledges support from the Paul M. Cook career development chair, the American Chemical Society's Petroleum Research Fund (Grant No. PRF 44106-G6), NSF Grant No. CHE-0547877, and the Packard Foundation. J.S.E. acknowledges helpful discussions with Qin Wu and Oleg Vydrov.

[1] T. A. Jung, R. R. Schlittler, J. K. Gimzewski, H. Tang, and C. Joachim, Science **271**, 181 (1996).
[2] L. A. Bumm, J. J. Arnold, M. T. Cygan, T. D. Dunbar, T. P. Burgin, L. Jones, D. L. Allara, J. M. Tour, and P. S. Weiss, Science **271**, 1705 (1996).
[3] M. A. Reed, C. Zhou, C. J. Muller, T. P. Burgin, and J. M. Tour, Science **278**, 252 (1997).
[4] B. C. Stipe, M. A. Rezaei, and W. Ho, Science **280**, 1732 (1998).
[5] G. Leatherman, E. Durantini, D. Gust, T. Moore, A. Moore, S. Stone, Z. Zhou, P. Rez, Y. Liu, and S. Lindsay, J. Phys. Chem. B **103**, 4006 (1999).
[6] H. Park, J. Park, A. K. L. Lim, E. H. Anderson, A. P. Alivisatos, and P. L. McEuen, Nature (London) **407**, 57 (2000).
[7] P. G. Collins, M. S. Arnold, and P. Avouris, Science **292**, 706 (2001).
[8] X. D. Cui, A. Primak, X. Zarate, J. Tomfohr, O. F. Sankey, A. L. Moore, T. A. Moore, D. Gust, G. Harris, and S. M. Lindsay, Science **294**, 571 (2001).
[9] P. McEuen, M. Fuhrer, and H. Park, IEEE Trans. Nanotechnol. **1**, 78 (2002).
[10] W. Liang, M. P. Shores, M. Bockrath, J. R. Long, and H. Park, Nature (London) **417**, 725 (2002).
[11] J. Park *et al.*, Nature (London) **417**, 722 (2002).
[12] P. Avouris, Acc. Chem. Res. **35**, 1026 (2002).
[13] J. Kushmerick, J. Lazorcik, C. Patterson, R. Shashidhar, D. Seferos, and G. Bazan, Nano Lett. **4**, 639 (2004).
[14] X. Xiao, B. Xu, and N. Tao, Nano Lett. **4**, 267 (2004).
[15] N. Guisinger, M. Greene, R. Basu, A. Baluch, and M. Hersam, Nano Lett. **4**, 55 (2004).
[16] R. McCreery, Chem. Mater. **16**, 4477 (2004).
[17] K. Kitagawa, T. Morita, and S. Kimura, J. Phys. Chem. B **109**, 13906 (2005).
[18] R. P. Andres, T. Bein, M. Dorogi, S. Feng, J. I. Henderson, C. P. Kubiak, W. Mahoney, R. G. Osifchin, and R. Reifenberger, Science **272**, 1323 (1996).
[19] R. Martel, T. Schmidt, H. R. Shea, T. Hertel, and P. Avouris, Appl. Phys. Lett. **73**, 2447 (1998).
[20] J. Chen, M. A. Reed, A. M. Rawlett, and J. M. Tour, Science **286**, 1550 (1999).
[21] M. C. Hersam, N. P. Guisinger, J. Lee, K. Cheng, and J. W. Lyding, Appl. Phys. Lett. **80**, 201 (2002).
[22] G. V. Nazin, X. H. Qiu, and W. Ho, Science **302**, 77 (2003).
[23] A. Salomon, D. Cahen, S. Lindsay, J. Tomfohr, V. Engelkes, and C. Frisbie, Adv. Mater. (Weinheim, Ger.) **15**, 1881 (2003).
[24] D. I. Gittins, D. Bethell, D. J. Schiffrin, and R. J. Nichols, Nature (London) **408**, 67 (2000).
[25] S. Wu, N. Ogawa, G. Nazin, and W. Ho, J. Phys. Chem. C **112**, 5241 (2008).
[26] N. J. Tao, Nat. Nanotechnol. **1**, 173 (2006).
[27] L. Venkataraman, J. E. Klare, C. Nuckolls, M. S. Hybertsen, and M. L. Steigerwald, Nature (London) **442**, 904 (2006).
[28] C. Livermore, C. H. Crouch, R. M. Westervelt, K. L. Campman, and A. C. Gossard, Science **274**, 1332 (1996).
[29] L. Yu, K. Chen, J. Song, J. Wang, J. Xu, W. Li, and X. Huang,

Thin Solid Films **515**, 5466 (2007).
[30] X. W. Tu, G. R. Mikaelian, and W. Ho, Phys. Rev. Lett. **100**, 126807 (2008).
[31] P. Liljeroth, J. Repp, and G. Meyer, Science **317**, 1203 (2007).
[32] R. Landauer, IBM J. Res. Dev. **1**, 223 (1957).
[33] R. Landauer, Philos. Mag. **21**, 863 (1970).
[34] R. Landauer, Z. Phys. B **21**, 247 (1975).
[35] M. Buttiker, Phys. Rev. Lett. **57**, 1761 (1986).
[36] M. Buttiker, Phys. Rev. B **38**, 9375 (1988).
[37] Y. Meir and N. S. Wingreen, Phys. Rev. Lett. **68**, 2512 (1992).
[38] L. Kadanoff and G. Baym, *Quantum Statistical Mechanics*, Reprint ed. (Westview, Boulder, 1994).
[39] V. Mujica, M. Kemp, and M. A. Ratner, J. Chem. Phys. **101**, 6849 (1994).
[40] M. P. Samanta, W. Tian, S. Datta, J. I. Henderson, and C. P. Kubiak, Phys. Rev. B **53**, R7626 (1996).
[41] L. E. Hall, J. R. Reimers, N. S. Hush, and K. Silverbrook, J. Chem. Phys. **112**, 1510 (2000).
[42] S. Datta, Superlattices Microstruct. **28**, 253 (2000).
[43] T. N. Todorov, J. Phys.: Condens. Matter **14**, 3049 (2002).
[44] P. Delaney and J. C. Greer, Phys. Rev. Lett. **93**, 036805 (2004).
[45] J. Taylor, H. Guo, and J. Wang, Phys. Rev. B **63**, 245407 (2001).
[46] P. Derosa and J. Seminario, J. Phys. Chem. B **105**, 471 (2001).
[47] Y. Xue, S. Datta, and M. A. Ratner, Chem. Phys. **281**, 151 (2002).
[48] M. Brandbyge, J. L. Mozos, P. Ordejon, J. Taylor, and K. Stokbro, Phys. Rev. B **65**, 165401 (2002).
[49] S.-H. Ke, H. U. Baranger, and W. Yang, Phys. Rev. B **70**, 085410 (2004).
[50] T. Tada, M. Kondo, and K. Yoshizawa, J. Chem. Phys. **121**, 8050 (2004).
[51] G. C. Solomon, J. R. Reimers, and N. S. Hush, J. Chem. Phys. **121**, 6615 (2004).
[52] G. C. Solomon, J. R. Reimers, and N. S. Hush, J. Chem. Phys. **122**, 224502 (2005).
[53] V. Mujica, M. Kemp, A. Roitberg, and M. Ratner, J. Chem. Phys. **104**, 7296 (1996).
[54] H. Ness and A. J. Fisher, Phys. Rev. Lett. **83**, 452 (1999).
[55] T. Kostyrko and B. R. Bulka, Phys. Rev. B **67**, 205331 (2003).
[56] C.-L. Cheng, J. S. Evans, and T. V. Voorhis, Phys. Rev. B **74**, 155112 (2006).
[57] E. Runge and E. K. U. Gross, Phys. Rev. Lett. **52**, 997 (1984).
[58] G. Stefanucci and C.-O. Almbladh, Europhys. Lett. **67**, 14 (2004).
[59] K. Burke, R. Car, and R. Gebauer, Phys. Rev. Lett. **94**, 146803 (2005).
[60] M. D. Ventra and T. N. Todorov, J. Phys.: Condens. Matter **16**, 8025 (2004).
[61] R. Baer, T. Seideman, S. Ilani, and D. Neuhauser, J. Chem. Phys. **120**, 3387 (2004).
[62] S. Kurth, G. Stefanucci, C.-O. Almbladh, A. Rubio, and E. K. U. Gross, Phys. Rev. B **72**, 035308 (2005).
[63] N. Bushong, N. Sai, and M. DiVentra, Nano Lett. **5**, 2569 (2005).
[64] F. D. M. Haldane, J. Phys. C **14**, 2585 (1981).
[65] E. A. Jagla, K. Hallberg, and C. A. Balseiro, Phys. Rev. B **47**, 5849 (1993).
[66] C. Kollath, U. Schollwock, and W. Zwerger, Phys. Rev. Lett. **95**, 176401 (2005).
[67] M. Polini and G. Vignale, Phys. Rev. Lett. **98**, 266403 (2007).
[68] C. Kollath and U. Schollwck, New J. Phys. **8**, 220 (2006).
[69] A. Recati, P. O. Fedichev, W. Zwerger, and P. Zoller, Phys. Rev. Lett. **90**, 020401 (2003).
[70] L. Kecke, H. Grabert, and W. Hausler, Phys. Rev. Lett. **94**, 176802 (2005).
[71] T. Stoferle, H. Moritz, C. Schori, M. Kohl, and T. Esslinger, Phys. Rev. Lett. **92**, 130403 (2004).
[72] B. Paredes, A. Widera, V. Murg, O. Mandel, S. Folling, I. Cirac, G. V. Shlyapnikov, T. W. Hansch, and I. Bloch, Nature (London) **429**, 277 (2004).
[73] C. Kollath, U. Schollwock, J. von Delft, and W. Zwerger, Phys. Rev. A **71**, 053606 (2005).
[74] K. Hallberg, A. A. Aligia, A. P. Kampf, and B. Normand, Phys. Rev. Lett. **93**, 067203 (2004).
[75] S. Akhanjee and Y. Tserkovnyak, Phys. Rev. B **76**, 140408(R) (2007).
[76] A. A. Zvyagin, Low Temp. Phys. **30**, 729 (2004).
[77] W. P. Su, J. R. Schrieffer, and A. J. Heeger, Phys. Rev. Lett. **42**, 1698 (1979).
[78] J. L. Bredas, R. R. Chance, and R. Silbey, J. Phys. Chem. **85**, 756 (1981).
[79] J. L. Bredas, R. R. Chance, and R. Silbey, Phys. Rev. B **26**, 5843 (1982).
[80] R. R. Chance, D. S. Boudreaux, J. L. Bredas, and R. Silbey, Phys. Rev. B **27**, 1440 (1983).
[81] D. S. Boudreaux, R. R. Chance, J. L. Bredas, and R. Silbey, Phys. Rev. B **28**, 6927 (1983).
[82] J. L. Bredas and G. B. Street, Acc. Chem. Res. **18**, 309 (1985).
[83] S. Stafstrom and K. A. Chao, Phys. Rev. B **29**, 2255 (1984).
[84] S. Stafstrom and K. A. Chao, Phys. Rev. B **30**, 2098 (1984).
[85] A. Terai and Y. Ono, J. Phys. Soc. Jpn. **55**, 213 (1986).
[86] H. Wendel, P. Otto, M. Seel, and J. Ladik, Solid State Commun. **54**, 551 (1985).
[87] W. Forner, C. L. Wang, F. Martino, and J. Ladik, Phys. Rev. B **37**, 4567 (1988).
[88] Z. G. Soos and S. Ramasesha, Phys. Rev. Lett. **51**, 2374 (1983).
[89] S. Mazumdar, S. Ramasesha, R. T. Clay, and D. K. Campbell, Phys. Rev. Lett. **82**, 1522 (1999).
[90] J. Pouget and S. Ravy, Synth. Met. **85**, 1523 (1997).
[91] T. Sasaki and N. Toyota, Phys. Rev. B **49**, 10120 (1994).
[92] M. V. Kartsovnik, A. E. Kovalev, I. F. Schegolev, V. N. Laukhin, N. D. Kushch, H. Ito, T. Ishiguro, G. Saito, and H. Mori, Synth. Met. **70**, 811 (1995).
[93] Y. Iye, R. Yagi, N. Hanasaki, S. Kagoshima, H. Mori, H. Fujimoto, and G. Saito, J. Phys. Soc. Jpn. **63**, 674 (1994).
[94] J. Caulfield, J. Singleton, P. T. J. Hendriks, J. A. A. J. Perenboom, F. L. Pratt, M. Doporto, W. Hayes, M. Kurmoo, and P. Day, J. Phys.: Condens. Matter **6**, L155 (1994).
[95] K. Miyagawa, A. Kawamoto, and K. Kanoda, Phys. Rev. B **56**, R8487 (1997).
[96] H. Jiang, H. U. Baranger, and W. Yang, Phys. Rev. Lett. **90**, 026806 (2003).
[97] H. Wang and Garnet Kin-Lic Chan, Phys. Rev. B **76**, 193310 (2007).
[98] S.-H. Ke, H. U. Baranger, and W. Yang, J. Chem. Phys. **126**, 201102 (2007).
[99] N. Sai, M. Zwolak, G. Vignale, and M. Di Ventra, Phys. Rev. Lett. **94**, 186810 (2005).
[100] C. Toher and S. Sanvito, Phys. Rev. Lett. **99**, 056801 (2007).
[101] C. Toher, A. Filippetti, S. Sanvito, and K. Burke, Phys. Rev.

Lett. **95**, 146402 (2005).
[102] M. Koentopp, K. Burke, and F. Evers, Phys. Rev. B **73**, 121403(R) (2006).
[103] S. Kummel, L. Kronik, and J. P. Perdew, Phys. Rev. Lett. **93**, 213002 (2004).
[104] S.-H. Ke, H. U. Baranger, and W. Yang, J. Chem. Phys. **122**, 074704 (2005).
[105] T. N. Todorov, G. A. D. Briggs, and A. P. Sutton, J. Phys.: Condens. Matter **5**, 2389 (1993).
[106] M. Zhuang and M. Ernzerhof, J. Chem. Phys. **120**, 4921 (2004).
[107] F. Zahid, M. Paulsson, E. Polizzi, A. W. Ghosh, L. Siddiqui, and S. Datta, J. Chem. Phys. **123**, 064707 (2005).
[108] F. Goyer, M. Ernzerhof, and M. Zhuang, J. Chem. Phys. **126**, 144104 (2007).
[109] M. Ernzerhof and M. Zhuang, J. Chem. Phys. **119**, 4134 (2003).
[110] P. Damle, A. W. Ghosh, and S. Datta, Chem. Phys. **281**, 171 (2002).
[111] S. Kohler, J. Lehmann, and P. Hanggi, Phys. Rep. **406**, 379 (2005).
[112] Q. Wu and T. V. Voorhis, Phys. Rev. A **72**, 024502 (2005).
[113] Q. Wu and T. Van Voorhis, J. Chem. Theory Comput. **2**, 765 (2006).
[114] E. Gross, J. Dobson, and M. Petersilka, *Density Functional Theory of Time-Dependent Phenomena* (Springer, Berlin, 1996), pp. 81–172.
[115] M. Paulsson and S. Stafstrom, Phys. Rev. B **64**, 035416 (2001).
[116] S. K. Pati, J. Chem. Phys. **118**, 6529 (2003).
[117] B. Muralidharan, A. W. Ghosh, and S. Datta, Phys. Rev. B **73**, 155410 (2006).
[118] R. Pariser and R. G. Parr, J. Chem. Phys. **21**, 466 (1953).
[119] J. A. Pople, Trans. Faraday Soc. **49**, 1375 (1953).
[120] K. Nishimoto and N. Mataga, Z. Phys. Chem., Neue Folge **12**, 335 (1957).
[121] N. Mataga and K. Nishimoto, Z. Phys. Chem., Neue Folge **13**, 140 (1957).
[122] J. P. Perdew and A. Zunger, Phys. Rev. B **23**, 5048 (1981).
[123] R. Baer and D. Neuhauser, J. Chem. Phys. **125**, 074709 (2006).
[124] Q. Wu and T. Van Voorhis, J. Phys. Chem. A **110**, 9212 (2006).
[125] I. Rudra, Q. Wu, and T. V. Voorhis, J. Chem. Phys. **124**, 024103 (2006).
[126] R. Baer, E. Livshits, and D. Neuhauser, Chem. Phys. **329**, 266 (2006).
[127] K. Capelle and E. K. U. Gross, Phys. Rev. Lett. **78**, 1872 (1997).
[128] K. Capelle, G. Vignale, and B. L. Györffy, Phys. Rev. Lett. **87**, 206403 (2001).
[129] I. Gerber and J. Angyan, Chem. Phys. Lett. **415**, 100 (2005).
[130] O. A. Vydrov, J. Heyd, A. V. Krukau, and G. E. Scuseria, J. Chem. Phys. **125**, 074106 (2006).